IMPROVING DISCHARGE CAPACITY OF SILICON ANODES BY REINFORCING MWCNTs USING HIGH SPEED PLANETARY BALL MILLING

T. Cetinkaya*, M. O. Guler, H. Akbulut

Sakarya University, Engineering Faculty, Department of Metallurgical & Materials Engineering, Esentepe Campus, 54187, Sakarya/TURKEY
**e-mail adress: tugrulcetinkaya@gmail.com*

Keywords: Si/MWCNT, mechanical alloying, cyclically test, impedance

Abstract
Silicon/multi-walled carbon nanotube powders (MWCNT) were mechanically alloyed by high energy mechanical milling (HEMM) method. Produced Si/MWCNT composite powders were prepared as an electrode with pasting on copper foil. Mechanically alloyed powders were characterised via X-ray diffraction technique (XRD) and scanning electron microscopy (SEM). CR2016 button type coin cells were prepared with using silicon/MWCNT composite electrodes. These cells discharge capacity cyclically tested by a battery tester at a constant current (300 mA/g) in voltage range between 0.05 V – 1.5 V. Furthermore, impedance values of cells were measurement before discharge and interphase electronic contact resistivity and solid electrolyte interface resistivity of electrodes were described.

1. Introduction
Rechargeable lithium ion batteries have revolutionized portable electronic devices. They have become the dominant power source for cell phones, digital cameras, laptops, etc., because of their superior energy density (capability to store 2–3 times the energy per unit weight and volume compared with conventional rechargeable batteries). The worldwide market for rechargeable lithium batteries is now valued at 10 billion dollars per annum and growing. They are the technology of choice for future hybrid-electric vehicles, which are central to the reduction of CO_2 emissions arising from transportation [1]. Commercial lithium-ion batteries usually adopt graphite as anode materials, whose theoretical capacity is only 372 $mAhg^{-1}$ (LiC_6). This low capacity of graphite anode is obviously insufficient to new generation portable electronics and the electric vehicles (EVs) or hybrid EVs [2]. Silicon is a promising candidate as a negative electrode in lithium-ion batteries due to its large theoretical energy density (about 4200 mAh g^{-1}, ten times higher than graphite) and relatively low working potential (~0.5 V vs Li/Li+). Currently, its use is frustrated by comparatively poor capacity retention and irreversible morphological change due to mechanical degradation caused by large changes in volume associated with lithiation/delithiation (~400%) during cycling [3]. To overcome this mechanical degradation and improve the electrochemical behaviour of silicon anodes, more attention has been paid silicon nanoparticles, silicon nanowires, and silicon based active composite anode materials with using carbon material such as graphite, carbon nanotube and graphene, etc. [4-8]. Carbon nanotube may find use in a wide range of applications in material reinforcement such as field emission panel display, chemical sensing,

drug delivery, and nanoelectronics due to structural perfection small size, low density, high stiffness, high strength (the tensile strength of the outer most shell of MWCNT is approximately 100 times greater than that of aluminium), and excellent electronic properties [9]. Carbon nonotubes (CNT) are known to have electrical resistances as low as metals (i.e., 2×10^{-4} to 3×10^{-4} Ωcm) and their ability to insert Li ions might allow them to be used as an anode active material. Moreover, their large aspect ratio may be helpful in retaining the conduction bridges when the composite swells [10, 11].

In this study, silicon/MWCNT composite were mechanically alloyed in PAN solution by using high speed planetary ball milling. Although there are investigations on the CNT reinforced silicon anode materials for Li-ion batteries, the mechanisms and the optimization of the CNT amount is not well understood. The aim of this work is firstly optimize the HEMM and then to coat on the MWCNT surfaces with a core-shell structure to increase discharge capacity of silicon nanocomposite anodes. The aim is extended to investigate the effect of MWCNT content in the nanocomposite to benefit the buffering effect of MWCNTs against mechanical disintegration caused from the large-volume increase of silicon during intercalation with lithium.

2. Experimental Methods

MWCNT (purity %95, diameter 50-100nm, length 10μm) used as reinforcing material for producing Si/MWCNT composites, in this study, supplied from Arry Nano. In order to purification, MWCNTs were stirred in HNO_3 for 12 hours, and then they were washed with water and dried overnight in an oven. Silicon particles (purity % 99.5, 130 nm in size) supplied from Nanostructured & Amorphous Materials Inc.. Polyacrynitrile (PAN, molecular weight 150,000) used in this study supplied from Sigma-Aldrich to avoid cold welding of silicon particles and excessive heating of silicon and MWCNT powders during the mechanical alloying process. Four different types of composites were prepared with using silicon powders, MWCNTs and PAN solution. For preparing PAN solution, 0.6 g PAN was dissolved in 10 ml N-methyl-2-pyrrolidinone (NMP) solution. Prepared PAN solution, different amount of MWCNTs and silicon powders were charged to bowl in argon filled glove box (~0.5 ppm oxygen and ~0.5 ppm moisture). Amount of PAN was kept constant for all composites composition. The four types of prepared composite compositions of resulting mixture and mechanical alloying process parameters is shown in Table 1 and as can be seen on Table 1, these composites were labelled as SP, SCP1, SCP2 and SCP3 type composites. These mixtures were mechanically milled for 1 hour using planetary ball mill (Fritsch, Pulverisette 7) to provide mechanical alloying between silicon and MWCNT powders. 80 ml stainless steel bowl and 5 mm balls were used for mechanical alloying process and ball to powder weight ratio 10:1. After mechanical alloying process, mixtures were dried at 150 ^{o}C for 10 hour and then subsequently isothermally annealed at 800 ^{o}C with a heating rate 5 ^{o}C min^{-1} for 4 h to decompose of PAN to form PAN-based carbon in flowing argon medium by using a quartz tube furnace. Phase constituents of powders were recorded on a Rigaku Dmax 2200 X-ray Diffraction Patterns (XRD) technique used Cu Kα radiation. Composite surface morphologies were observed with Jeol 6060 LV Scanning Electron Microscopy (SEM). To investigate of PAN decomposition temperature, TGA analyses were carried out in argon environment. For preparation of electrodes, 75 wt.% mechanically milled active composite powders and 10 wt.% carbon black mixed with 15 wt.% PVDF binder dissolved in N-methyl-2-pyrrolidinone (NMP) solution. The resulting slurry was cast on a copper foil and pasted by doctor blade coating technique and dried at 120 ^{o}C in the vacuum oven for 12 h. After then sample on copper foil 16 mm in diameter was cut. Coin type CR2016 test cells were

assembled in argon filled glove box, the prepared electrodes were used as an working electrode, Li foil used as counter electrode and 1M $LiPF_6$ dissolved in a mixture of ethylene carbonate (EC) and diethyl carbonate (DEC) (1:1 in volume) as the electrolyte. The working and counter electrodes were separated with polypropylene (PP) separator. Charge–discharge characteristics were obtained at 293 K between 0.05 V and 1.5 V at a constant current of 300 mA/g. Moreover, EIS of produced electrodes were measurement in frequency range 1000 kHz to 10 mHz with AC amplitude of 10 mV using Gamry Instrument Version 5.67.

Composition of starting material (wt.%)	Samples	Milling speed (rpm)
70 Si - 30 PAN	SP	700
10 MWCNT - 60 Si - 30 PAN	SCP1	700
20 MWCNT - 50 Si - 30 PAN	SCP2	700
30 MWCNT - 40 Si - 30 PAN	SCP3	700

Table 1. Mechanical alloying parameters for producing silicon/MWCNT composite.

3. Results and Discussions

Fig. 1a shows XRD patterns of pan-based carbon (PAN-C), purified MWCNTs, raw-silicon, SP type composite, SCP1 type composite, SCP2 type composite and SCP3 type composite powders. On the other hand, Fig. 1b demonstrates low angle XRD patterns of raw- silicon, SP, SCP1, SCP2 and SCP3 type composites. It can be seen that PAN-C has quasi crystalline structure and these quasi crystalline peaks were observed as carbon peaks reflection at 2θ values of ≈ 26°, 44° and 51° in SP type composite. When the amount of MWCNTs increase, carbon peaks reflection intensity does not change due to high amorphous structure of CNT. Furthermore, silicon carbide (SiC) phase which has an inactive behavior against lithium [12] is not detected in composite structures. Fig. 1b demonstrates the highest plane (111) of silicon, and it is clearly seen when the amount of MWCNTs increase, silicon reflection peak is shifted towards to the lower 2θ region and plane spacing of $d_{(111)}$ is increased from 3,144 Å to 3,153 Å. Won I. Park et al. [13] who studied fabrication and photoluminescent properties of heteroepitaxial ZnO/$Zn_{0.8}Mg_{0.2}O$ coaxial nanorod heterostructures and found that dominant peak of ZnO shift in XRD patterns due to lattice strain of ZnO when ZnO nanorod coat with $Zn_{0.8}Mg_{0.2}O$. H. J. Chae et al. [14] who studied the physicochemical characteristics of pillared interlayered clays and reported that when introduce pillar particles between basal planes, basal plane of clay shifted towards to lower 2θ region. According to this review, it is possible to say when the amount of MWCNT increases, silicon particles show lattice strain and silicon particles indicate deformation due to introducing MWCNT in silicon structure.

Fig. 2 shows scanning electron microscopy images of silicon powders and multi-wall carbon nanotubes (MWCNTs). SEM micrograph in Fig. 2a belongs to raw-silicon powders that used as matrix material in composite structure. Fig. 2b, on the other hand, represents the purified MWCNTs used for reinforcing material. High and low magnification SEM images of SP, SCP1, SCP2 and SCP3 composites are shown in Fig. 3. Fig. 3a and 3b belong to SP type composite, Fig. 3c and 3d represent SCP1 type composite, Fig. 3e and 3f demonstrate SCP2 type composite and Fig. 3g, and 3h indicate SCP3 type composite powders surface morphology. SEM micrographs of SP type composite in Fig. 3. show that silicon powders to have slight agglomeration due to PAN-based carbon network [15]. At low magnification, SEM images of SCP1 type composite structure, it cannot be clearly understood whether the silicon powders are dispersed in composite. However, at high magnification, SEM image of SCP1 type composite shows silicon powders are settled down on the surface of MWCNTs and strongly combined with MWCNT surface. When the amount of MWCNTs is increased

(SCP2 and SCP3 type composites, respectively), silicon particles are observed as effectively coated on the MWCNTs surfaces. The reason for settled silicon particles on MWCNTs surfaces can be caused from PAN-based carbon effect. Because, PAN-based carbon enhancing the interface adhesion/bonding between Si and carbon [17]. The other reason can be etching of MWCNTs in nitric acid solution before mixing with silicon powders. It is possible that nitric acid creates some active sites on MWCNTs surface and silicon particles located these active sites on the surface of MWCNTs. As mentioned in XRD results, when the amount of MWCNT increases, silicon particles show lattice strain and deformation due to introducing MWCNT in silicon structure. SEM micrographs are clearly agreed with this comment. Because, silicon powders are strongly coated on MWCNT surface due to introducing MWCNT in structure with increasing amount of MWCNT.

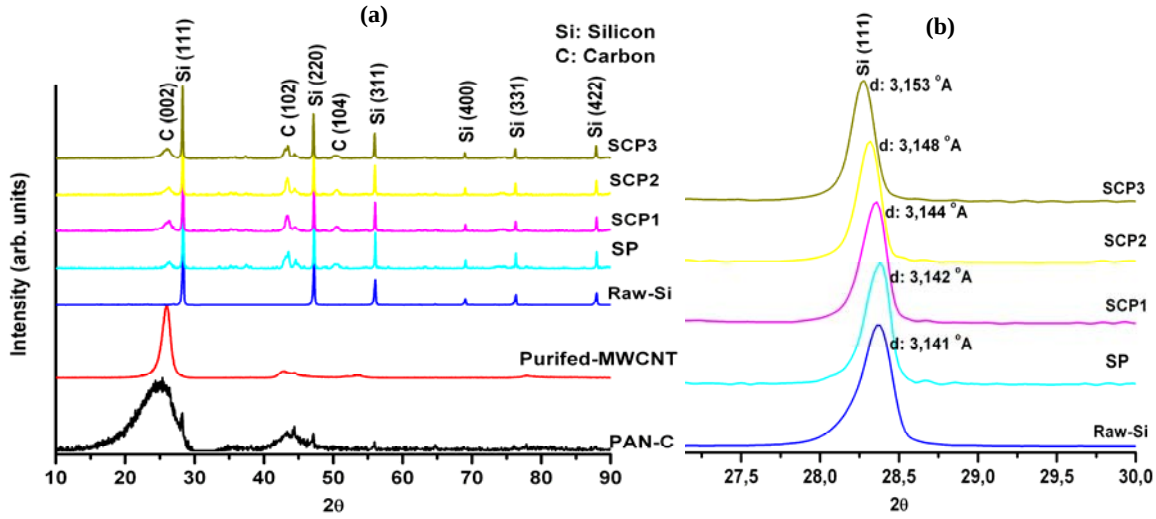

Figure 1. a) x-ray diffraction patterns of PAN-C, purified-MWCNT, raw-si, SP type composite, SCP1 type composite, SCP2 type composite and SCP3 type composite, b) low angle x-ray diffraction patterns of raw-si, SP, SCP1, SCP2 and SCP3 type composites.

In order to identify weight loss of PAN, TGA has been performed for pure-PAN in the argon environment in Fig. 4a. Furthermore, TGA has been performed for SP, SCP1, SCP2 and SCP3 type composite in air to determine the weight content of silicon in composite in Fig. 4b. TGA results of PAN shows a significant weight loss (73 wt. %) at 800 °C, which corresponds to decomposition PAN to form PAN-based carbon in Fig. 4a [16]. TGA results of carbonized SP, SCP1, SCP2 and SCP3 composite demonstrate to contain of SP type composite 89 wt.% silicon, SCP1 type composite contains 75 wt.% silicon, SCP2 type composite contains 65 wt.% silicon, SCP3 type composite contains 50 wt.% silicon. The weight increase after 700 °C in the TGA curves of SP, SCP1, SCP2 and SCP3 composite is due to the oxidation of Si in air above 700°C [15].

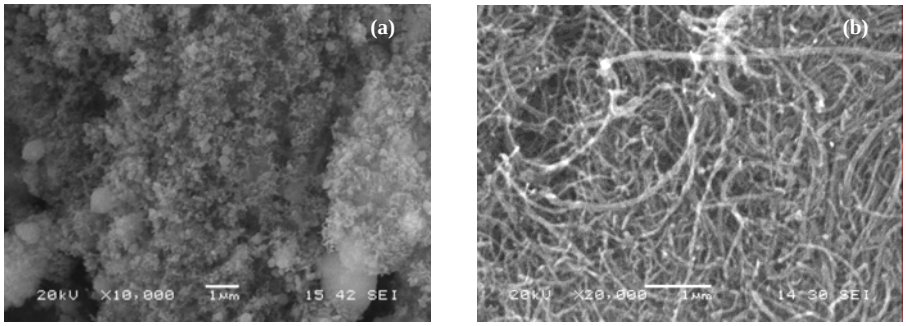

Figure 2. SEM images of a) raw-silicon particles and b) purified multi-wall carbon nanotubes.

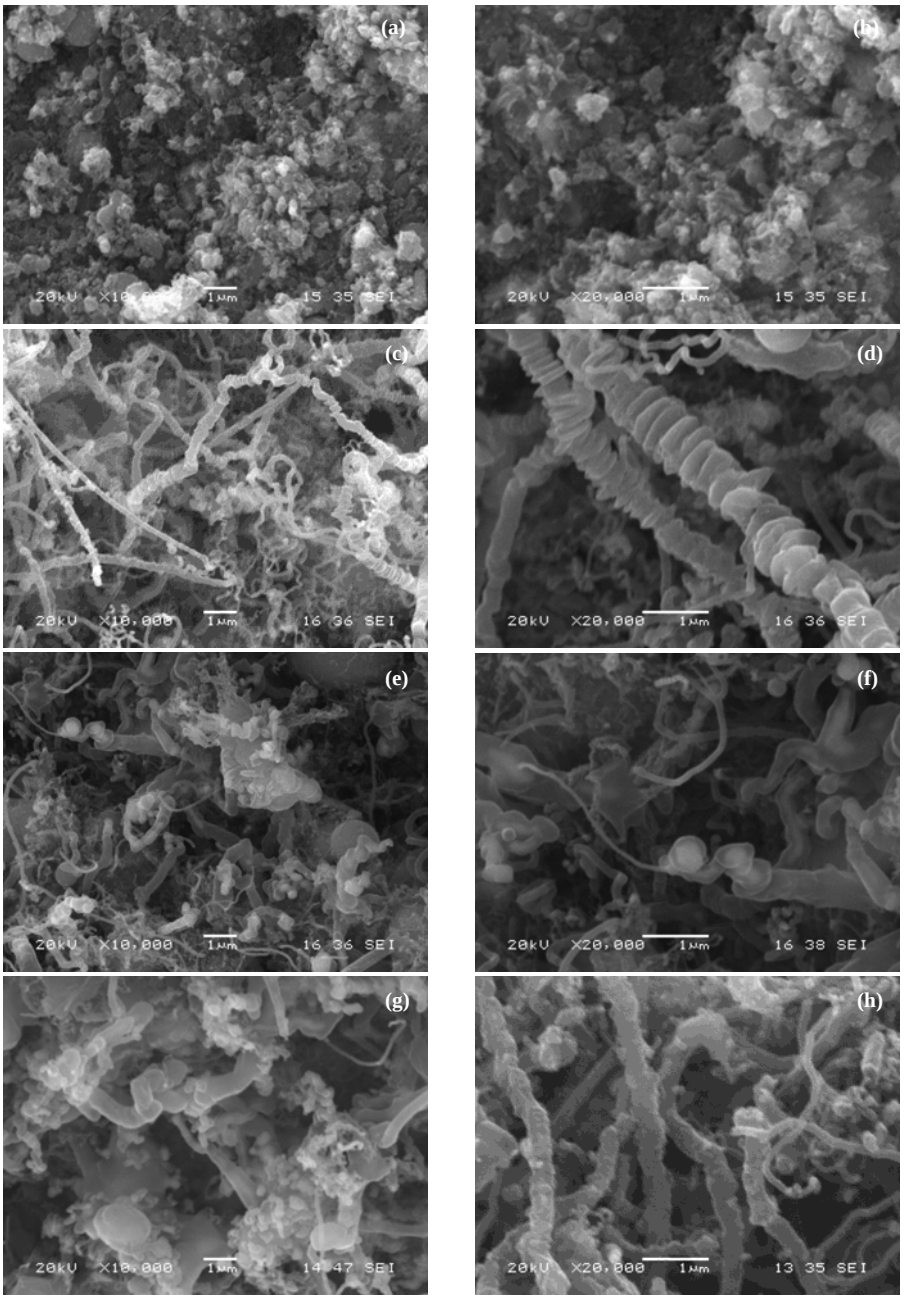

Figure 3. Low and high magnifications SEM images; a) and b) SP type composite, c) and d) SCP1 type composite, e) and f) SCP2 type composite, g) and h) SCP3 type composite structures.

To investigate the effect of MWCNT on electric resistance of electrodes, EIS of electrodes was measured. EIS measurements of electrodes are shown in Fig. 5a. The Fig. 5b shows equivalent circuit for impedance spectra of SP, SCP1, SCP2 and SCP3 type composites. This equivalent circuit consists of a series of three resistors and constant phase elements (CPE) in parallel. The symbols of R_S, R_2 and R_3 denoted the solid electrolyte interphase (SEI) resistance (high frequency semicircle), interphase electronic contact resistance (low frequency semicircle) and charge transfer resistance (middle frequency semicircle). The fitted impedance using this equivalent circuit agrees well with the impedance spectra in Fig. 5a. By fitting the impedance data, SEI resistance and interphase electronic contact resistance was obtained and showed in Fig. 6. As can be seen from Fig. 6a interphase electronic contact resistance decreases with increasing amount of MWCNT. X. Li et al. [17] who studied a novel network composite cathode of LiFePO4/multiwalled carbon nanotubes with high rate

capability for lithium-ion batteries and reported $LifePO_4$/MWCNT composite electronic conductivity of the composite cathode was improved with adding MWCNT. Our work clearly agrees with the findings obtained by X. Li et al. Fig. 7b shows SEI resistance, which corresponds to high irreversible capacity at the first lithium insertion and extraction cycle [18], and it is seen that highest SEI resistance was found on SP type composite electrode and lowest SEI resistance were observed on SCP3 type composite electrode.

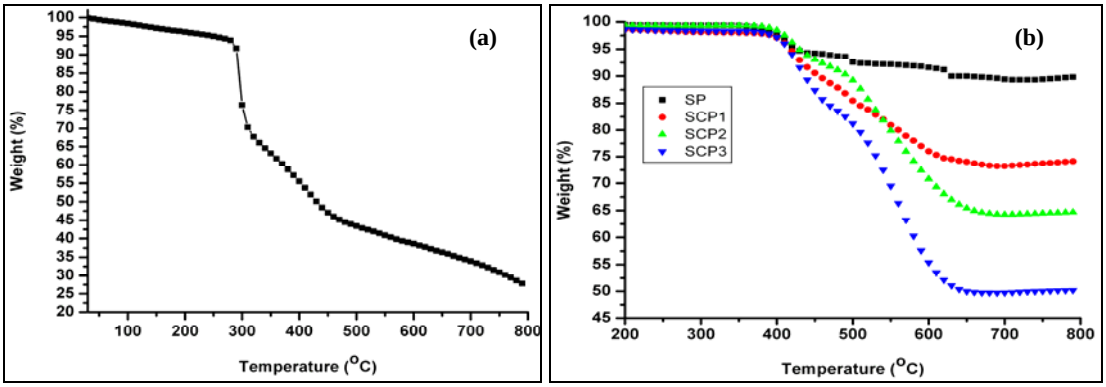

Figure 4. TGA curves of a) the pure PAN conducted in high purity argon, b) the carbonized Si/MWCNT composite in air.

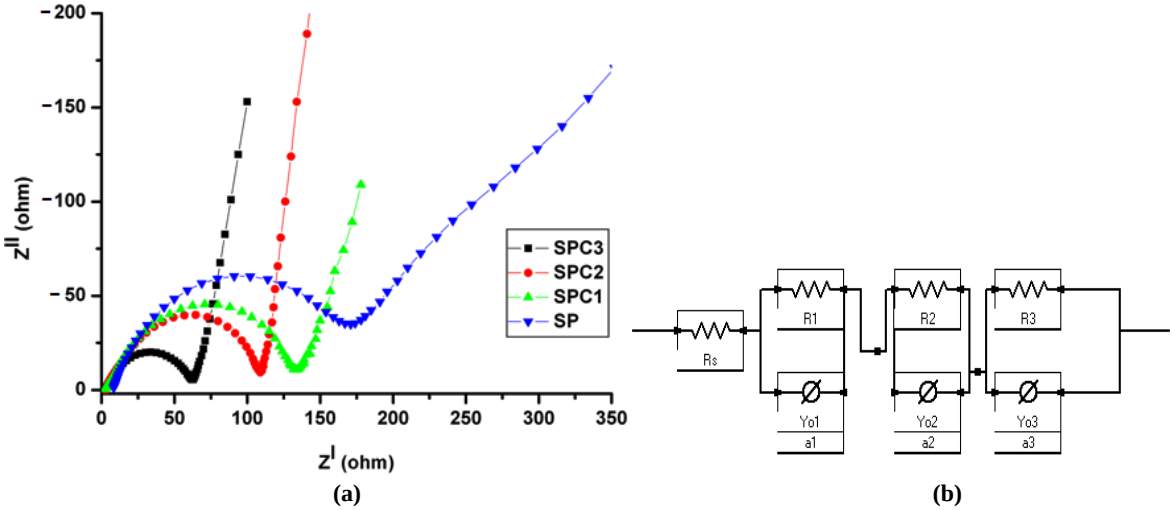

Figure 5. a) Impedance spectra of produced electrodes and b) Equivalent circuit of used to model the impedance spectra.

The discharge capacities of produced electrodes up to 50th cycle are shown in Fig 7a. The charge/discharge current was 300 mAh/g based on silicon weight. First discharge capacity of SP type composite is 3200 mAh/g, SCP1 type composite is 1586 mAh/g, SCP2 type composite 1125mAh/g and SCP3 type composite is 1324mAh/g. In SP type composite, discharge capacity drop to approximately 740 mAh/g on 10th cycle. J. Guo et all [16] reported that adding MWCNT increase capacity in the early stage and our SCP1 and SCP2 type composites clearly agree with J. Guo's report. However, in SCP3 type composite which including about 38 wt.% MWCNT after the carbonization show almost stable discharge capacity during all cycles. This capacity retention was seen for silicon nano wire in literature [6]. Because the active material silicon particles were strongly coated on the surface of MWCNT in SCP3 type composite and owing to hollow, high flexible structure of MWCNTs, it can be easily suggested that the SCP3 type composite can tailor the volume increase because of lithium interstation to the silicon anode. Since the MWCNTs can also behave as load carrying agents which, is well described for fiber reinforced composites the mechanical

disintegration and associated high electrochemical performances. As mentioned in impedance spectra, SCP3 type composite has the highest interphase electronic conductivity and lowest SEI resistance. These results can be attributed to high capacity retention of SCP3 type composite. In order to demonstrate capacity retention of SCP3 type composite electrodes, charge/discharge curve of SCP3 type composite up to 20th cycle is shown in Fig. 7b, and this curve explains capacity retention of SCP3 type composite during cycling.

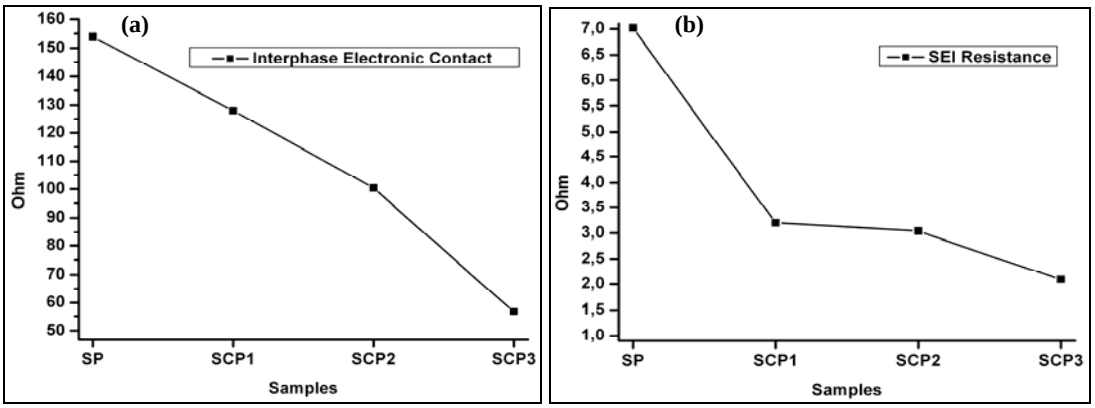

Figure 6. Produced electrodes a) interphase electronic contact resistance, b) SEI resistance.

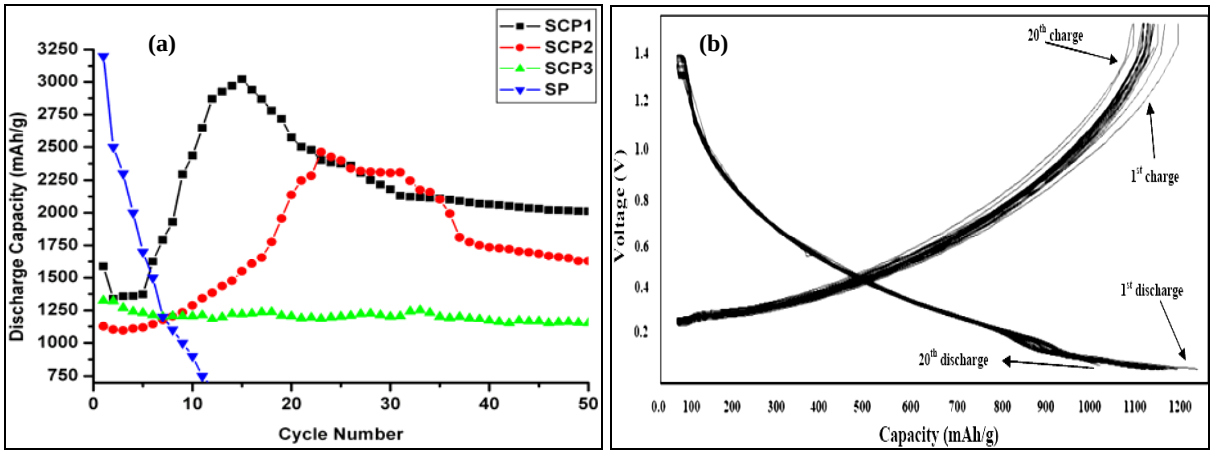

Figure 7. a) Cycling test of SP, SCP1, SCP2 and SCP3 type electrodes and b) charge/discharge profile of SCP3 type composite.

4. Conclusions

1. MWCNT reinforced silicon electrodes were successfully produced by HEMM method without significant MWCNT agglomeration.
2. Increasing MWCNT content in the silicon matrix results in coating silicon nano grains onto MWCNTs and produces core-shell like structure.
3. Increasing MWCNT content caused in lattice strain increment and shifting silicon reflection peaks towards to the lower 2θ values and increasing spacing between crystal planes.
4. Introducing MWCNTS into silicon resulted in discharge capacity increment and better capacity retention in comparison with unreinforced silicon.
5. Increasing MWCNT content into silicon produced very high discharge capacities. The cell assembled with 30 wt. % MWCNT reinforced silicon anode yielded 1151 mAh/g discharge capacity even at 50 cycles.
6. Highest SEI resistance was found in unreinforced silicon anode and lowest SEI resistances obtained in the 30 vol. % MWCNT reinforced silicon nanocomposite electrode.

Acknowledgement
This work is supported by the Scientific and Technological Research Council of Turkey (TUBITAK) under the contract number 111M021. The authors thank the TUBITAK MAG workers for their financial support.

References
[1] Bruce P., Scrosati B., Tarascon J. M., Nanomaterials for rechargeable lithium ion baterries, Angew. *Chem. Int. Ed*, **47**, pp. 2930 – 2946, 2008.
[2] Peng B., Cheng F.,Tao Z., Chen J., Lithium transport at silicon thin film: Barrier for high-rate capability anode, *The Journal of Chemical Physics*, **133**, pp. 034701-5, 2010.
[3] Song T., Xia J., Lee J. H., Lee D. H., Kwon M. S. et all, Arrays of sealed Silicon nanotubes as anodes for lithium ion batteries, *Nano Letters*, **10**, 1710–1716, 2010.
[4] Ding N., Xu J., Yao Y., Wegner G., Lieberwirth I., Chen C., Improvement of cyclability of Si as anode for Li-ion batteries, *Journal of Power Sources*, **192**, 644–651, 2009.
[5] Chakrapani V., Rusli F., Filler M. A., Kohl P. A., Silicon nanowire anode: Improved battery life with capacity-limited cycling, *Journal of Power Sources*, **205**, pp. 433–438, 2012.
[6] Dimov N., Kugino S., Yoshio M., Mixed silicon–graphite composites as anode material for lithium ion batteries Influence of preparation conditions on the properties of the material, *Journal of Power Sources*, **136**, pp. 108–114, 2004.
[7] Wang W., Kumta P. N., Nanostructured Hybrid Silicon/Carbon Nanotube Heterostructures: Reversible High-Capacity Lithium-Ion Anodes, *ACS Nano*, **4**, pp. 2233-2241, 2010.
[8] Lee J. K., Smith K. B., Hayner, Kung H. K, Silicon nanoparticles–graphene paper composites for Li ion battery anodes, *Chem. Commun*., **46**, pp 2025–2027, 2010.
[9] Qian D., Wagner G. J., Liu W. K., Yu M. F., Ruoff R. S., Mechanics of carbon nanotubes, *Appl. Mech. Rev.*,**55**, pp. 495-533, 2002.
[10] Sheem K., Lee Y. L., Lim H. S., High-density positive electrodes containing carbon nanotubes for use in Li-ion cells, *Journal of Power Sources*, **158**, pp. 1425–1430, 2006.
[11] Varzi A.,Täubert C., Mehrens M. W., Kreis M., Schütz W., Study of multi-walled carbon nanotubes for lithium-ion battery electrodes, *Journal of Power Sources*, **196**, pp. 3303–3309, 2011.
[12] Wang X., Wen Z., Liu Y., Xu X., Lin J., Preparation and characterization of a new nanosized silicon–nickel–graphite composite as anode material for lithium ion batteries *Journal of Power Sources*, **189**, pp. 121–126, 2009.
[13] Park W. I., Yoo J., Kim D. W., Yi G. C., Fabrication and Photoluminescent Properties of Heteroepitaxial ZnO/Zn0.8Mg0.2O Coaxial Nanorod Heterostructures, *J. Phys. Chem. B*, **110** ,pp. 1516-1519, 2006.
[14] Chae H. J.,Nam I. S., Ham S. W., Hong S. B., Physicochemical characteristics of pillared interlayered clays, *Catalysis Today*, **68**, pp. 31–40, 2001.
[15] Guo J., Sun A., Chen X., Wang C., Manivannan A., Cyclability study of silicon–carbon composite anodes for lithium-ion batteries using electrochemical impedance spectroscopy Electrochimica Acta, **56**, pp. 3981–3987, 2011.
[16] Datta M. K., Kumta P. N., Silicon and carbon based composite anodes for lithium ion batteries, *Journal of Power Sources*, **158**, pp. 557–563, 2006.
[17] Li X., Kang F., Bai X., Shen W., A novel network composite cathode of LiFePO4/multiwalled carbon nanotubes with high rate capability for lithium ion batteries, *Electrochemistry Communications*, **9**, pp. 663–666, 2007.
[18] Si Q., Hanai K., Ichikawa T., Hirano A., Imanishi N., Takeda Y., Yamamoto O., A high performance silicon/carbon composite anode with carbon nanofiber for lithium-ion batteries *Journal of Power Sources*, **195**, 1720–1725, 2010.